Journal of Engineering Physics and Thermophysics, Vol. 72, No. 3, 1999

BUBBLE GROWTH RATE AND PHENOMENON OF DEGENERATE BOILING OF A FLUID IN THE FORM OF FILM VAPORIZATION

A. R. Dorokhov and V. I. Zhukov

UDC 536.423.1

An analysis of results of an investigation of vaporization of a thin fluid film under vacuum is presented. The vaporization process has basic features characteristic of bubble boiling of a fluid, except for formation of bubbles. This makes it possible to classify the phenomenon as degenerate boiling of a fluid in the form of film evaporation during which local thinning of the layer takes place and funnel- and crater-shaped structures are formed. Funnels and craters are vapor sources with different powers. Dependences of the bubble growth rate above vapor sources of both types that generalize available experimental data are obtained.

The relationship between the heat transfer in bubble boiling of fluids and the bubble growth mechanism in boiling in an infinitely large volume of superheated fluids has been rather thoroughly investigated. In theoretical consideration of the problem and in generalization of results of experimental investigations, solutions for the radius of a growing bubble are usually obtained in the following form [1]:

$$R_b = A_b t^n, \tag{1}$$

where R_b is the bubble radius, A_b is a constant, and $n = 1/2 - 1$.

New information on the relationship between the heat-transfer mechanism and bubble growth mechanisms on a heating surface can be obtained in investigation of certain cases with limiting values of the heat-transfer parameters. One of them is presented in experimental investigations of heat transfer in thin fluid films under vacuum [2]. No bubble formation was observed in the layer; however, several microlayer zones of different shapes and other phenomena characteristic of bubble-boiling processes were observed. Whereas bubble growth usually takes place in several tens of microseconds, the phenomena noted in in [2] had a duration of several seconds (several thousand microseconds), and they could be observed with the unaided eye and were recorded using a conventional photocamera. A preliminary analysis of the results obtained in conformity with an investigation of the growth rate of vapor bubbles on the heating surface in boiling was carried out in [3].

The working chamber where the experiments were carried out consisted of a casing in the form of a cylinder with an inner diameter $d = 120$ mm and a height of 300 mm made of stainless steel. A cooling coil (with water as the coolant) was situated on the outer surface of the upper portion of the cylinder. The temperature was measured by copper-constantan thermocouples made of 0.12 mm wire. The pressure in the volume was measured by a U-shaped oil differential manometer and was controlled by a valve. A more detailed description of the experimental setup can be found elsewhere [2].

Prior to the experiments, a certain amount of liquid (vacuum mineral oil VM-1) was poured on the bottom to provide a layer of the required thickness. The oil was degassed by boiling under vacuum for 6-8 h. Visual observations were made through windows in the upper and lower portions of the chamber. Processes in the layer were photographed using a Zenith-TTL camera with the exposure set at 1/30 sec.

It should be pointed out that in using conventional visualization methods for investigation of the boiling process, the information required can be obtained only with the use of a high-speed photographic technique.

Novosibirsk State Technical University, Novosibirsk, Russia. Translated from Inzhenerno-Fizicheskii Zhurnal, Vol. 72, No. 3, pp. 458-465, May-June, 1999. Original article submitted January 20, 1998.

 1062-0125/99/7203-0430$22.00

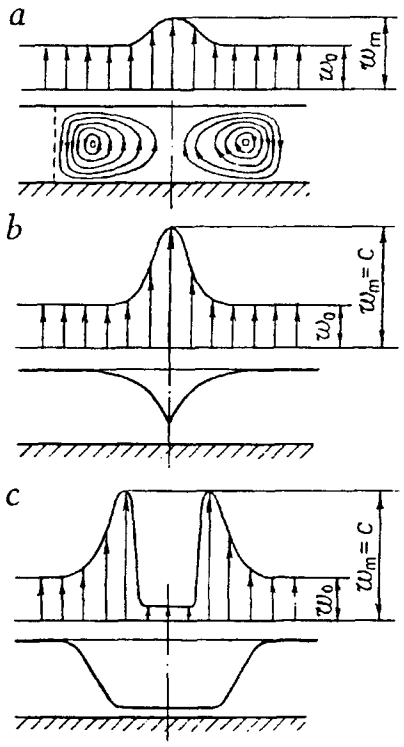

Fig. 1. Crater formation dynamics: a) convective cell; b)funnel; c) crater.

The most detailed observations were carried out for an oil layer with a height of 2 mm. In one case, the pressure was set at 200 Pa, and in the other case, measurements were set at 5–10 Pa. Explosive boiling took place at a pressure of 200 Pa, whereas at 5–10 Pa it was absent, and the process schematically presented in Fig. 1 was observed.

Figure 1a presents a cross section of a convective cell with flow lines shown. A schematic view of the velocity profile of the liquid vapor is presented. Warmer liquid rises in the center, and cooler liquid descends at the edges. A temperature gradient usually exists at the free boundary of convective cells [4]. When the liquid is heated almost to its boiling point, intense vaporization of it from the free upper boundary sets in. At this instant, the reactive force of the phase transition has different values in differently heated surface regions. In regions where the liquid is warmer, it has higher values [5], and under its effect the liquid layer is thinned here, and a funnel is formed (Fig. 1b). The funnels move over the surface and disappear at the walls of the chamber, where cooler condensed liquid flows down. The existence of the funnels is maintained by the reactive force of the phase transition. The fog jets that flow out of the funnels, visually observed in transmitted light, indicate that the liquid evaporation rate is higher on the funnel surface than in other regions. The funnel moves over the chamber bottom from a cooler region that is cooled as a result of vaporization from the funnel base to a hotter one. Visual observations revealed no vapor bubbles in the liquid upon formation of funnels. In warmer regions, the density of funnels is higher. Here, craters covered with an oil microlayer are formed (Fig. 1c). The craters move over the surface. The trajectories of funnel motion mostly coincide with drift trajectories of convective cells. The craters have arbitrary trajectories of motion. It need only be noted that not a single crater passed twice over one and the same point of the heating surface.

Figure 2 presents photographs of the processes observed in an oil film of thickness 2 mm. In the region over which a crater has passed, which has resulted in cooling of the liquid due to intense evaporation, first no ordered motions in the oil are observed, and then convective cells appear in the layer. After a time, funnels appear at their sites (Fig. 2a). In the region where the funnel density is highest, a crater is formed again (Fig. 2b). The process is repeated; the number, size, and rate of formation of craters increase with the specific heat flux. In certain cases, at the instant when the crater is formed, the liquid at its edges is raised a little by the vapor flow escaping from under the layer. The duration of crater motion over the surface is 1–3 sec. Over the entire range of variation of the heat flux, when the regime of coexistence of funnels and craters was realized, the latter were covered with

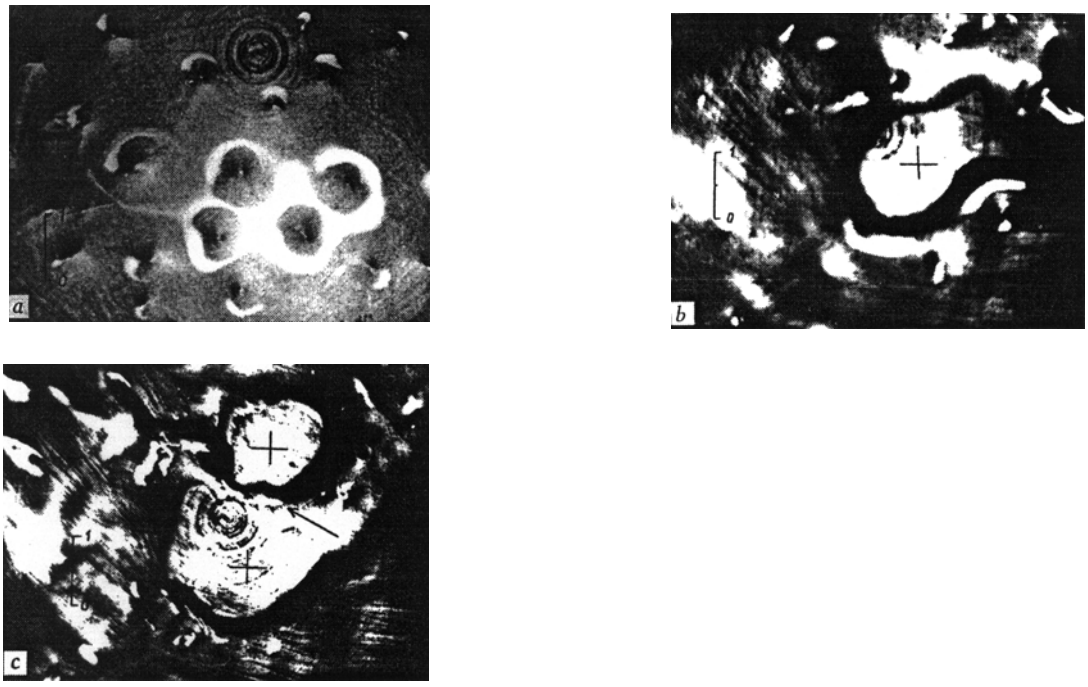

Fig. 2. Photographs of processes observed in a film of VM-1 oil of thickness 2 mm: a) funnel; b) crater (shown by the cross); c) two craters connected by a bridge (shown by the arrow). Scale 1 cm.

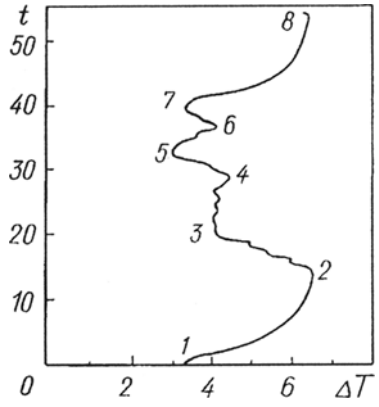

Fig. 3. Surface-temperature pulsations during boiling of a film in the range of low heat fluxes. t, sec; ΔT, K.

an oil microlayer. Finally, at high specific heat fluxes, a regime appears in which much of the surface is covered with craters wetted by narrow oil bridges moving between them (Fig. 2c). At heat fluxes corresponding to the onset of this regime, the craters remain covered by an oil microlayer. When the heat flux increases further, the microlayers on the crater surfaces begin to vaporize instantaneously, which is followed by washing-out of the crater by the oil bridge.

In the experiments, the temperature of the heating surface was measured by a thermocouple situated at a distance of 0.1 mm from the surface. Readings of the thermocouple were recorded by an automatic recorder. Figure 3 shows changes in the surface temperature in an oil layer of height 2 mm at a specific heat flux $q \sim 10{,}000$ W/m^2 in the case where a pressure of 5–10 Pa was maintained prior to heating. At the initial instant, no clusters are observed in the layer, and the temperature of the heating surface grows exponentially (segment 1-2). After $t \sim 15$ sec, craters appear in the layer, and the surface temperature decreases (segment 2-3), and then it remains almost constant for a certain time (segment 3-4). At the instant $t \sim 27$ sec, a crater passes over the thermocouple mounted in the bottom of the cylinder, and the temperature of the bottom decreases sharply (segment 4-5), and

then it increases (segment 5-6). The next peak in this curve corresponds to passage of the next crater (segment 6-7). At $t \sim 40$ sec, the temperature of the surface starts to grow exponentially again to its original level as craters start to appear in the layer (segment 7-8). The instant of passage of a crater over the thermocouple site was detected visually.

By its form of manifestation (the absence of vapor bubbles), the process observed differs from conventional boiling of liquids, and therefore, in [2] we classified it as evaporation, which indeed takes place. However, this process has features in common with conventional bubble boiling of liquids:

1) upon an increase in the heat flux, it changes regimes of convective heat transfer and is much more intense compared to the latter;

2) pulsations of the surface temperature are observed under the structures (funnels and craters) formed during the process;

3) a liquid microlayer is formed on the surface (at the base of funnels and craters).

In addition, in boiling of a liquid under vacuum, phenomena similar to the above-outlined process have been observed, namely, motion of bubbles over the heating surface [6] that is similar to the motion of craters. Taking into account the above features, one can classify the process as a phenomenon of degenerate boiling of a liquid in the form of film vaporization that consists in the fact that in heating from below a thin liquid layer on a horizontal heating surface under vacuum, local thinning of the layer occurs and structures in the form of funnels (Fig. 2a) and moving craters (Fig. 2b) appear that are caused the action of the reactive force of the phase transition, which is nonuniformly distributed over the upper boundary of the liquid layer. Let us consider the properties of the structures.

The shape of the funnels remains constant under certain external conditions in the bulk and on the heating surface. The shape of the craters changes during their motion over the surface. The trajectories of funnel motion coincide with those of drift of convective cells over the heating surface. Individual craters have different nonintersecting trajectories of motion.

Funnels and craters appear in the regions of the most intense liquid vaporization, and therefore, they can be considered as sources of vapor, and a thermal characteristic such as the vapor source power Q can be introduced to describe them.

Funnels exist at low heat fluxes, and craters cover the entire heating surface at high heat fluxes, from which it follows that the funnel power Q_f is lower than the power of craters Q_c. The question of why funnels (low-energy structures) are replaced by craters (high-energy structures) arises. What limits the heat flux removed by funnels?

First, funnels have well-defined dimensions under given conditions in the bulk, and therefore it is evident that there exists a limiting surface density of funnels N, and thus the heat flux removed by funnels from a unit area cannot exceed $q = NQ_f$.

Second, the power of an idividual funnel Q_f is also limited under certain conditions in the bulk. Let us return to the discussion of the process presented schematically in Fig. 1. When the layer is heated in the regime of convective heat transfer, vapor leaves the upper boundary of the layer with the velocity w_0 (Fig. 1a). The heat flux removed from the surface of the liquid layer is therefore $Q = r\rho_v w_0 S$.

Then funnels are formed on the surface of the liquid layer (Fig. 1b). In the center of a funnel, the liquid layer has the smallest thickness and the heat-transfer coefficient and the temperature have the lowest values, and therefore the velocity of vapor escape has the maximum value w_m in this region. Liquid with the lowest temperature vaporizes on the upper boundary, and therefore the velocity of vapor escape in this region has the lowest value w_0. The velocity profile of the vapor over the funnel radius can be represented in the form

$$w - w_0 = (w_m - w_0) f(\eta),$$

where $f(\eta)$ is an axisymmetric function that varies from unity at the funnel center to zero on the upper boundary of the liquid layer. The value of the function $f(\eta)$ drops rapidly with distance from the funnel center, and the

(unknown) temperature distribution over the funnel surface is required for calculation of the function. The funnel power is as follows:

$$Q_f = \rho_v r 2\pi \int_0^{R_f} wydy = \rho_v r (w_m - w_0) 2\pi R_f^2 \int_0^1 f(\eta)\eta d\eta + \rho_v r w_0 \pi R_f^2,$$

which, after transformations, takes the following form:

$$Q_f = \rho_v r w_m \pi R_f^2 \left[(1 - w_0/w_m) 2 \int_0^1 f(\eta)\eta d\eta + w_0/w_m \right].$$

Let us analyze the expression obtained. The funnel shape is determined by the effect of the reactive force of the phase transition – actually, by the ratio w_0/w_m, where w_0 determines the effect of the reactive force of the phase transition on the upper boundary of the liquid layer, and w_m that on the funnel's bottom. Since the funnel shape remains constant at a constant pressure in the bulk, $w_0/w_m = \text{const}$ and $\int_0^1 f(\eta)\eta d\eta = \text{const}$. The funnel radius, vapor density, and heat of the phase transition can also be considered to be constant. Then

$$Q_f = r\rho_v w_m \pi R_f^2 \text{ const} = A w_m.$$

It follows from the expression obtained that the power of a funnel is directly proportional to the velocity of vapor escape from its bottom. The vapor escape velocity is bounded by the propagaton velocity of small perturbations, i.e., the velocity of sound $c = \sqrt{\gamma RT/M}$. When the temperature of the heating surface changes by several degrees, e.g., from $T_1 = 520$ K to $T_2 = 530$ K (as in experiments [2]), the velocity of sound changes insignificantly: $\sqrt{T_1/T_2} = 1.01$. At the same time, the heat flux supplied to the heating surface changes by several hundred percent. Therefore, funnels are vapor sources of constant power, $Q_f = \text{const}$. This conclusion does not contradict experimental findings [2] and makes it possible to explain why funnels are replaced by craters.

As the heat flux grows, the corresponding increase in the heat transfer is attained by means of an increase in the number of funnels on the surface. The funnels appear in hotter regions of the surface, and some work is spent on their creation. The existence of this work of funnel creation makes it possible to stabilize the heat-transfer process in the regions with the maximum superheating and thus to prevent the appearance of craters in these regions. When the limiting population density of funnels on the liquid surface is attained, the liquid cannot be cooled further through the funnel surfaces. Therefore, a further increase in the heat flux in the layer leads to the appearance of craters.

As opposed to the funnels, the craters (Fig. 1c) do not have constant shape and dimensions. Their appearance is accompanied by emergence of pressure pulsations in the bulk, and therefore, the craters are variable-power vapor sources. The crater power is a sum of two components: $Q_c = Q_w + Q_p$, where Q_w is the heat flux removed from the crater surface covered with an oil microlayer, and Q_p is the heat flux removed from the meniscus at the interface between the heating surface and the liquid. When the crater is formed, the most intense vaporization of the liquid takes place in the vicinity of the meniscus. In this region, the liquid is pushed away due to the effect of the reactive force emerging as a result of the phase transition. In regions where the vaporization front has passed, the liquid cools down [2], and therefore vaporization of the liquid on the cold crater surface can be neglected. Thus, one can consider the crater power to be determined by the vapor flow escaping from the meniscus region, i.e., $Q_c = Q_p$. The velocity of vapor escape in the case of craters is also limited by the velocity of sound c.

The qualitative regularities of the process are the same for boiling of liquids under different conditions. If this takes place in a large volume, (funnel-type) constant-power vapor sources can be observed at the small heat fluxes at the start of the boiling curve, when bubbles from different vaporization centers do not merge and there exist enough vaporization centers to preclude explosion-type boiling. The power of vapor sources Q can be calculated from the bubble growth rate. The equation for the change in the bubble volume V is as follows:

$$\rho_v r\,(dV/dt) = Q\,. \tag{2}$$

In the case of a constant-power vapor source, $Q = Q_f = \text{const}$, and then the following formula for the change in the bubble radius holds:

$$R_{b,f} = (3Q_f t/4\pi\,\rho_v r)^{1/3} = A_{b,f} t^{1/3}\,. \tag{3}$$

In [3], one of us compared experimental data obtained for the growth of bubbles in various liquids on heating surfaces of different materials with calculations by Eq. (3), and good coincidence was observed. In [7], it is pointed out that the growth of vapor bubbles in liquid metals also obeys dependence (3).

In the case of bubble growth over a (crater-type) variable-power vapor source, the source power Q_c is the sum of the heat flux supplied from the wall through the liquid microlayer at the bubble base Q_w, the heat flux supplied from the liquid Q_L, and the heat flux supplied from the meniscus at the bubble base Q_p:

$$Q_c = Q_w + Q_L + Q_p\,,$$

Due to the inhomogeneity of the temperature distribution in the wall layer, the most intense evaporation of the liquid takes place from a narrow evaporation layer of thickness x situated at the bubble-wall interface at the base of the bubble, i.e., from the meniscus. A cooling temperature wave is formed under the bubble, which moves into the bulk of the heating surface, which is followed by the reheating of the heating surface under the bubble. As is shown by observations [2], the microlayer is evaporated completely only at high heat fluxes in a regime where only craters are observed on the heating surface. Therefore, at slight superheating of the main body of the liquid, the heat fluxes Q_L and Q_w can be neglected. Then, in the period of bubble growth on the heating surface over a crater-type vapor source the power of the latter is $Q_c = Q_p$.

Let the condition $x << R_c$ be satisfied, then the area of the vaporization surface equals $S_c = 2\pi R_c x$. The specific heat flux of vaporization is $q_v = r\rho_v c$, and

$$Q_c = 2\pi R_c\, xr\,\rho_v c = S_c q_v\,.$$

For boiling of water at atmospheric pressure, we obtain $q_v = 6\cdot 10^8$ W/m^2. This evaluation coincides with results of calculations of [8] in order of magnitude and is several orders of magnitude higher than the heat flux supplied to the liquid from the heating surface, which leads to temperature pulsations under a growing bubble.

By inserting the expression for Q_c and the dependence of the bubble volume on its radius into heat-balance equation (2), we obtain

$$r\rho_v 4\pi R_{b,c}^2\,(dR_{b,c}/dt) = 2\pi R_c\, xr\,\rho_v c\,.$$

If viscosity effects and cooling of the liquid and the wall ahead of the evaporation front are neglected, one obtains a constant width of the evaporation front x, and one can write

$$2r\,\rho_v R_{b,c}^2\,(dR_{b,c}/dt) = R_c q_{v,p}\,,$$

where $q_{v,p}$ is the heat flux per unit length of the bubble base (meniscus) perimeter. If similarity of the linear dimensions of the bubble occurs at all instants of time (e.g., hemispherical bubbles), $R_c/R_{b,c} = f = \text{const}$, and then

$$2r\,\rho_v R_{b,c}^2\,(dR_{b,c}/dt) = R_c q_{v,p}\,,$$

from which a typical law for the growth of the bubble radius follows:

$$R_{b,c} = (q_{v,p}/2r\,\rho_v f^3)^{1/2}\, t^{1/2} = A_{b,c} t^{1/2}\,. \tag{4}$$

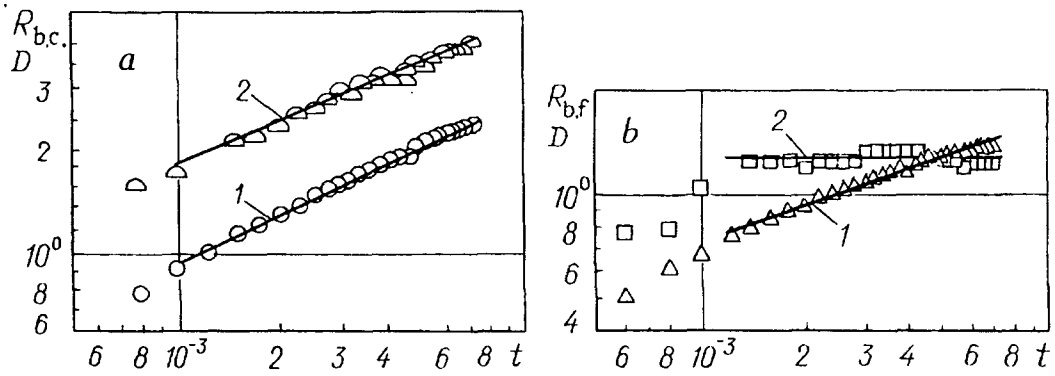

Fig. 4. Time dependences of the bubble radius (1) and the bubble base diameter (2) for bubbles growing over variable-power (crater) (a) and constant-power (funnel) (b) vapor sources. $R_{b,c}$, $R_{b,f}$, D, mm; t, sec.

Experimental data [9] were processed using the method of least squares. The exponent $n \sim 1/2$ in the bubble growth law (1) was obtained for the radius of hemispherical bubbles. Figure 4a presents a comparison of calculations with experimental data. Curve 1 shows the time dependence of the radius of a hemispherical bubble $R_{b,c} \approx t^{1/2}$, and curve 2 shows a similar dependence for the growth rate of the diameter of the base of a hemispherical bubble $D = 2R_c \sim t^{1/2}$. The coincidence of the results of the qualitative analysis with experimental data substantiates the validity of the above assumptions of a constant heat flux $q_{v,p}$. The estimate of the vaporization front width $x \sim 2$ μm is obtained for hemispherical bubbles from experimental data [9] on boiling of water at atmospheric pressure.

It should be pointed out that the volume V in heat-balance equation (2) can be evaluated from the equivalent bubble radius satisfying the relationship $R_{equ} = (3V/4\pi)^{1/3}$, where V is the volume of a bubble of arbitrary shape. Here, the value of the derivative dV/dt in the heat-balance equation does not change. In what follows, the bubble radius means its equivalent radius $R = R_{equ}$, and here $R_c = D/2$ is the actual geometric radius of the bubble base.

For funnel-type constant-power vapor sources, we obtained relationship (3), according to which $n \sim 1/3$ (curve 1 in Fig. 4b). Since after formation of a funnel its shape remains constant, the radius of the bubble base R_c should remain constant (curve 2 in Fig. 4b).

Let us consider the problem in the general formulation. Let $R_b = A_b t^n$ (Eq. (1)) and $R_c = A_c t^k$, and then, by inserting these relationships into (2) and carrying out corresponding cancellations, we obtain

$$2A_b^3 n t^{3n-1} = A_c t^k c x . \tag{5}$$

In the above analysis, $n = 1/2$ and $k = 1/2$ were obtained for crater-type variable-power vapor sources. For funnel-type constant-power vapor sources $n = 1/3$ and $k = 0$. By simple substitution in (5), one can show that the relationship $3n - 1 = k$ holds. Thus, for $1/2 \le n \le 1/3$, the time dependence in (5) can be excluded. Then we arrive at the identity $2A_b^3 n \equiv A_c c x$, from which it follows that the width of the vaporization front x remains constant for constant values of n over the entire range of n:

$$x = (2A_b^3 n / A_c c) .$$

It follows from experimental data [9] that $x \sim 1 - 2$ μm for boiling of water at atmospheric pressure. For crater-type variable-power vapor sources, the width of the vaporization front x is larger than for funnel-type constant-power vapor sources.

CONCLUSIONS

1. We have shown in this work that in vaporization of a liquid from a thin layer under vacuum [2], the main regularities inherent in the boiling process, except for formation of bubbles, are observed. Therefore, the phenomenon observed in [2] can be classified as degenerate boiling of a liquid in the form of film vaporization.

2. An analysis of degenerate boiling of a liquid in the form of film vaporization has revealed two types of vapor sources: funnels and craters – with constant and variable power, respectively.

3. An analysis of the reasons leading to a change from a boiling regime in which funnels (low-energy structures) prevail in the layer to a regime with craters (high-energy structures) prevailing in the layer leads to bounding of the velocity of vapor escape from the vaporizing liquid by the velocity of sound.

4. Equations (3) and (4) for bubble growth above vapor sources of both types are obtained, which generalize well existing experimental data on boiling of various liquids in a large volume.

5. It is shown that Eqs. (3) and (4) can be combined into a single common equation from which the width of the liquid vaporization front can be evaluated for boiling of water at atmospheric pressure.

The work was carried out within the framework of project No. 330 of FTsP Integratsiya.

NOTATION

A_i, constant in the law of structural-unit growth; D, diameter of the bubble base; M, molar weight; N, surface density of funnels; Q and Q_i, vapor-source power; R, gas constant; R_i, radius of structural unit; S, area of vaporization surface; T, temperature; V, bubble volume; c, velocity of sound; d, diameter of the working chamber; n, k, exponents; q_i, heat flux; r, heat of vaporization; t, time; w_i, vapor motion velocity; x, width of the vaporization front; y, current funnel radius; ρ_v, vapor density; $\eta = y/R_f$, dimensionless funnel radius; γ, adiabatic exponent. Subscripts: b, bubble; c, crater; f, funnel; m, maximum value; p, perimeter (meniscus); w, heating surface; v, vapor; 0, unperturbed flux; L, liquid; equ, equivalent.

REFERENCES

1. V. E. Nakoryakov and A. V. Gorin, Heat and Mass Transfer in Two-Phase Systems [in Russian], Novosibirsk (1994).
2. I. I. Gogonin, A. R. Dorokhov, and V. I. Zhukov, Izv. Sib. Otdel. Akad. Nauk SSSR, Ser. Tekh. Nauk, Issue 3, 8-13 (1989).
3. V. I. Zhukov, Pis'ma Zh. Tekh. Fiz., 22, Issue 21, 34-38 (1996).
4. V. S. Berdnikov and A. G. Kirdyashkin, Izv. Akad. Nauk SSSR, Fiz. Atmosfery Okeana, 15, No. 11, 1158-1174 (1979).
5. H. J. Palmer and J. C. Maheshri, Int. J. Heat Mass Transfer, 24, No. 1, 117-123 (1981).
6. V. I. Deev, V. V. Gusev, and G. P. Dubrovskii, Teploénergetika, No. 8, 73-75 (1965).
7. V. F. Prisnyakov, Boiling [in Russian], Kiev (1988).
8. Z. Guo and M. S. El-Genk, Int. J. Heat Mass Transfer, 37, No. 11, 1641-1655 (1994).
9. N. B. Hospeti and R. B. Mesler, AIChE J., 15, No. 2, 214-219 (1969).